IJNRD.ORG ISSN : 2456-4184
INTERNATIONAL JOURNAL OF NOVEL RESEARCH AND DEVELOPMENT (IJNRD) | IJNRD.ORG
An International Open Access, Peer-reviewed, Refereed Journal

Analyzing Crack Growth In Cylindrical Bars: A Comprehensive Research Using Finite Element Analysis

Pushpendra patel[1st] Prakash Pandey [2nd] S.S. Chauhan [3rd]
[1]Department of Machine Design, Vaishnavi Group of Institutions, Bhopal
[2]Department of Machine Design, Vaishnavi Group of Institutions, Bhopal
[3]Department of Machine Design, Vaishnavi Group of Institutions, Bhopal

Abstract: This research paper explores the complex realm of crack growth in cylindrical bars, focusing on the atomic-level phenomena involving the breakage and separation of atomic bonds and the movement of dislocations within the material structure. The study explores how new surfaces are formed in solids as cracks nucleate and expand due to applied loads. The paper discusses the adaptation of materials to critical levels of load and the factors leading to stable or unstable crack growth. Various fatigue life methods, including stress-life, strain-life, and linear-elastic fracture mechanics, are analyzed, and the paper investigates the impact of elliptical cracks on cylindrical bars using Finite Element Analysis (FEA). The research meticulously examines crack orientation angles, stress ratios, and loading sequences, shedding light on the complex behavior of cracks in real-world scenarios. The study also explores crack closure phenomena and presents mathematical models for predicting crack growth rates. Furthermore, the research emphasizes the crucial role of advanced coating layers, self-healing mechanisms, and non-destructive testing techniques in managing crack propagation.

Index Terms **- Crack Growth, Cylindrical Bars, Finite Element Analysis, Fatigue Life Methods, Elliptical Cracks, Stress Intensity Factor, Crack Closure, Non-Destructive Testing, Coating Layers, Self-Healing Mechanisms.**

I. INTRODUCTION

Crack growth is on the atomic level breakage and separation of the bonds linking the atoms and/or movement and gathering of dislocations (imperfections in the atomic structure). Thus, new surfaces are created in the solid as the crack nucleates and continues to grow. This can be interpreted as an adaption of the material to an applied load of a critical level. Application of a strictly increasing load to a flawed structure may not be critical at first since the load needs to be at some critical level in order for crack growth to occur. At this point stable or unstable crack growth occurs dependent on the characteristics of the material resistance to continuous growth and the driving force dependence vs crack extension. However, at some point, assuming a strictly increasing load, the component or structure will fail due to loss of load bearing capacity or functionality.

The cylindrical bars are widely used in machine components and structures. Surface cracks are generally found in the components due to applied cyclic loads, material defects and improper manufacturing processes. During service loading, the crack or flaw may propagate into a critical stage, resulting in an undesirable catastrophic failure. Therefore, it is necessary to analyze the crack behavior for proper diagnosis of fatigue failure.

1.1 Prediction of Life of a cracked part

The lifetime of a cracked part is typically expressed as the number of cycles that it takes to grow the crack from some initial condition to a critical condition. Generally it is necessary to use numerical methods to determine the expected lifetime of a part. In this case, the crack growth is simulated using the general procedure shown below.

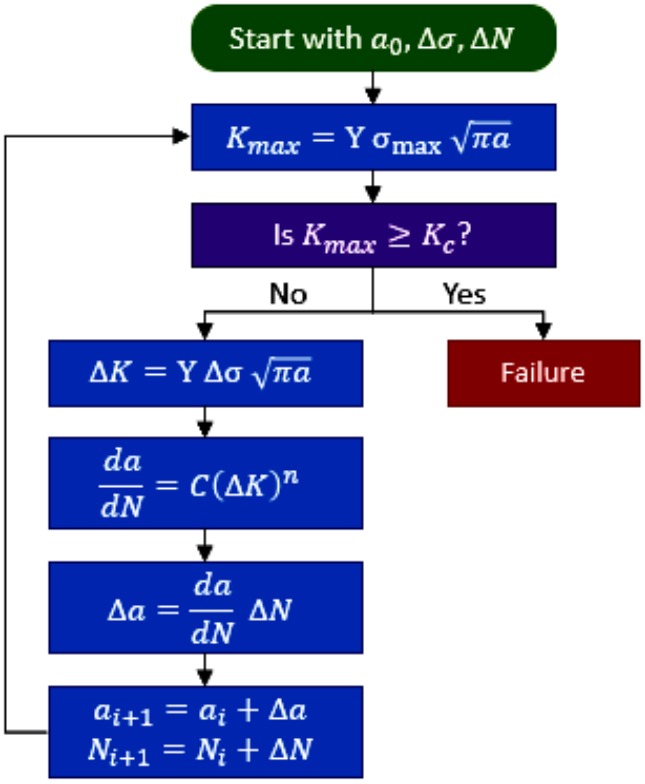

Figure 1 Expected lifetime of a part

1.2 Fatigue-Life Methods

The three major fatigue life methods used in design and analysis are

- Stress-life method,
- Strain-life method, and
- Linear-elastic fracture mechanics method.

Life of $1 \leq N \leq 10^3$ cycles is generally classified as low-cycle fatigue, whereas high-cycle fatigue is considered to be $N > 10^3$ cycles. The stress-life method, based on stress levels only, is the least accurate approach, especially for low-cycle applications. The strain-life method, while requiring a more intricate analysis of plastic deformation in localized regions, offers a valuable approach for assessing fatigue life, particularly in low-cycle fatigue applications. This method delves deeper into the intricacies of stress and strain, providing a more refined understanding of the material's behavior.

1.3 Fatigue Crack Growth

Cracks commonly occur in engineered parts and can significantly reduce their ability to withstand load. Cracks typically form around pre-existing flaws in a part. They usually start off small and then grow during operational use.

A crack in a part will grow under conditions of cyclic applied loading, or under a steady load in a hostile chemical environment. Crack growth due to cyclic loading is called fatigue crack growth.

1.4 Crack Size vs. Cycles

A typical plot showing the growth of a crack is provided below. The crack size, a, is shown as a function of cycles, N, of applied load. The rate of crack growth is $\frac{da}{dN}$ and is the instantaneous slope of the crack growth curve.

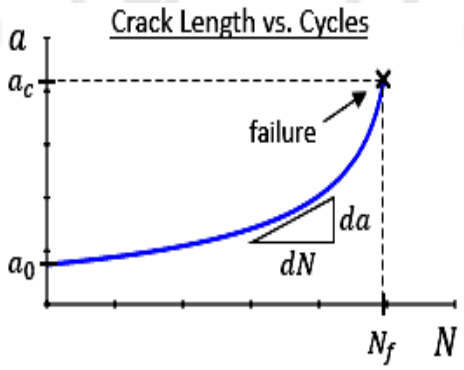

Figure 2 Crack length Vs number of cycles

Notice that the crack initially grows very slowly, but the growth accelerates (i.e. $\frac{da}{dN}$ increases) as the crack size increases. The reason for this acceleration in growth is that the growth rate is dependent on the stress intensity factor at the crack tip, and the stress

intensity factor is dependent on the crack size, a. As the crack grows the stress intensity factor increases, leading to faster growth. The crack grows until it reaches a critical size and failure occurs.

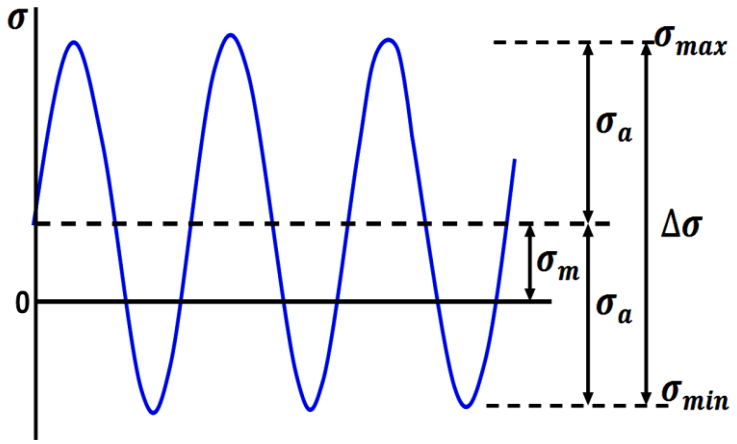

Figure 3 Reverse cyclic loading

Fracture Mechanics Theory

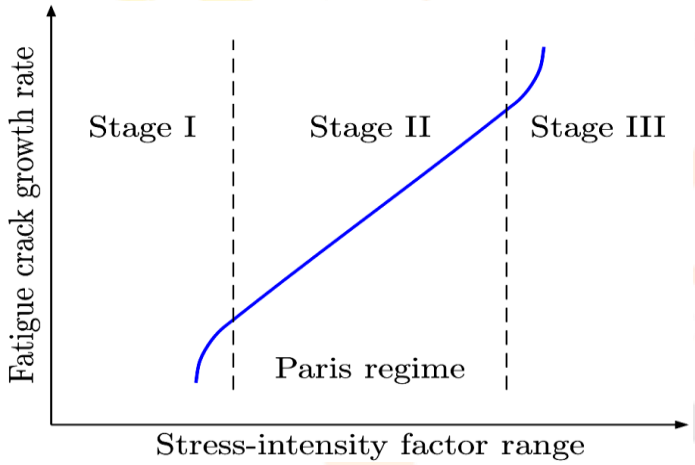

Figure 4 Fatigue crack growth rate Vs the stress-intensity factor range

The fracture mechanics theory is commonly used to characterize the severity of the applied load on the fatigue crack tip. If the plastic deformation at the crack tip due to the applied load is small relative to the characteristic dimensions of the geometry, then linear elastic fracture mechanics (LEFM) is applicable. The parameter used for the linear description of the load on the fatigue crack tip is called the stress-intensity factor, K_I. Numerous researchers have shown that the main factor controlling the propagation rate, in the case of fatigue crack propagation, is the range of the stress-intensity factor, ΔK_I.

Factors affecting crack growth rate

Regimes

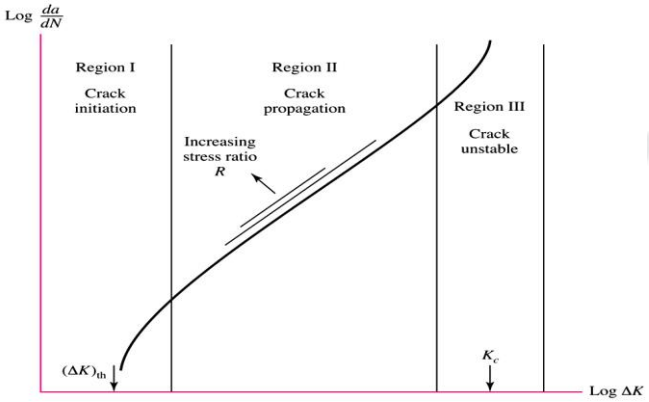

Figure 5 Crack growth regimes

II LITERATURE REVIEW

Yang Yua et al. (2021) [1] We propose a novel time-based approach for predicting fatigue damage in steel bridges, eliminating the need for cycle counting. This method leverages a comprehensive coupled vehicle-bridge interaction framework in full-scale, serving as the basis for numerical demonstrations. Initially, we conduct numerical simulations within this framework to generate stress time histories for a typical steel bridge under varying traffic loads. Subsequently, we employ the time-based fatigue crack growth (FCG) analysis method to assess the impact of road surface roughness and vehicle weight on FCG. Finally, we present a case study involving the I-10 Twin Span Bridge, showcasing the application of our time-based FCG method for fatigue damage prognosis using in situ monitoring data. Our findings affirm that this innovative approach enables the direct prediction of steel bridge FCG in the time domain, utilizing stress time histories derived from stress analysis or real-time in situ monitoring, with promising results for practical implementation and enhanced bridge maintenance strategies.

Z.K.Xuab et al. (2021) [8] In recent decades, researchers have noted that the fatigue crack growth rate in certain materials can be influenced by a zigzag crack growth path, although the underlying mechanism remained unclear. This study investigated the impact of crack growth paths on the fatigue crack growth rate in 18Ni maraging steel under three different heat treatment conditions, identifying two key factors at play. The primary factor was found to be the material's strength, while the zigzag crack growth path, rather than slowing down crack growth, was found to increase it. To gain a deeper understanding of this influence, a two-phase model was developed. In this model, different phases exhibit varying resistances to crack growth, and the difference in strength between these phases determines whether the zigzag path can mitigate or accelerate fatigue crack growth. Specifically, when the strength difference between the second phase and the matrix surpasses a certain threshold, the zigzag path accelerates fatigue crack growth. This research underscores that not all zigzag crack propagation paths contribute to enhanced fatigue cracking resistance, and a detailed analysis should consider the specific microstructure of the material.

William M.Williams et al. (2021) [9] The 3d transition metal high entropy alloy, CoCrFeNi, has demonstrated promising mechanical and corrosion resistance properties. In this study, CoCrFeNi underwent tension-tension fatigue testing at room temperature, allowing for an exploration of its steady-state fatigue crack growth behavior and the underlying deformation mechanisms. Notably, CoCrFeNi exhibited favorable resistance to steady-state fatigue crack growth, with its Paris law exponent falling at the lower end of the spectrum typical for ductile metals, approximately $m \approx 2.5$, irrespective of the load ratio. Through TEM analysis conducted at various locations, it was revealed that the plastic deformation mechanism shifted from dislocation slip to the introduction of nano-twinning as ΔK increased over the crack's lifecycle.

R.G.Pettit (2021) [10] In this research, we utilized an enhanced electrothermal pulsing method that offers superior current capability and more precise timing of pulses. By applying electrical pulses at high amplitude, we initiated cracks at significantly reduced loads. Moreover, to create visible indicators on the fracture surface for post-test analysis, we employed a lower amplitude pulse to heat tint the crack tip during the examination. Specifically, one marking was made under near-threshold conditions before concluding the threshold test to determine if this marking technique affects the outcomes. Notably, a minor, measurable artifact was detected right after marking under near-threshold conditions, which disappeared after a crack growth of .001-.003 inches. The data gathered from this study pertained to Ti 6-4 forging and Inconel 718 forging.

Kamleshwar Kumar et al. (2021) [13] Corrosion-induced material erosion often results in the formation of pits, which can act as stress risers, compromising structural integrity. To address and protect structures with these existing pitfalls, the finite element analysis (FEA) proves to be an invaluable tool. In our study, we have delved into the effects of pit shapes on crack initiation and subsequent propagation within a rectangular plate, employing the extended finite element method (XFEM) for our investigations. A range of pit designs were evaluated, including semi-circular, semi-elliptical, rectangular, and bullet-shaped pits. To accurately represent the material's damage behavior, we adopted the cohesive segment modeling approach. Our analysis further encompassed subjecting the rectangular plate to both tension and bending forces to ascertain their respective impacts on crack initiation. Our findings highlighted a significant observation: the shape and presence of pits play a pivotal role in determining crack initiation tendencies under both tensile and bending forces.

S.Japea et al. (2021) [14] Shape Memory Alloys (SMA) are unique materials whose actuation technology hinges on a comprehensive grasp of their behavioral response to "actuation" loading, which is primarily influenced by thermal variations. Our paper delves deep into this domain, revealing groundbreaking experimental insights into the stable crack growth of SMA compact tension specimens as they undergo temperature fluctuations while being under constant bias loads – a phenomenon hitherto unreported. Digging deeper into the intrinsic factors driving this crack progression, our findings align with the pre-established literature, pinpointing the combination of cleavage and ductile void growth, typical of nominally isothermal overload fractures, as the key damage mechanisms. To further validate and bolster our experimental observations, we've employed a rigorous numerical analysis. The consequent simulations were juxtaposed against the experimental findings, aiming to affirm and solidify the understanding of the extrinsic factors either enhancing or obstructing crack progression. One of the key takeaways from our research is the multifaceted role of phase transformation in influencing crack growth dynamics. Specifically, when phase transformation manifests as a fan before the crack tip, it acts as a catalyst, expediting crack progression. Conversely, when this transformation is observed in the aftermath of an advancing crack, it enhances the toughness of the material, ensuring the crack growth remains stable. This latter phenomenon, known as transformation-induced toughness enhancement, is widely recognized. However, the former, promoting crack growth, is a novel observation, especially in the context of SMAs exposed to actuation loading conditions.
Thanh Thuong et al. (2021) [15] The study delved into the impact of hydrogen on the features of crack growth in thin specimens, utilizing a thin sheet of single-crystal Fe-3wt%Si alloy for the purpose. We examined center-cracked samples in a hydrogen environment under sustained load and in an air environment under continuous stretching. This approach allowed for a comparison to understand hydrogen's role in delayed crack growth. Interestingly, despite the noticeable difference in specimen thickness, the crack growth mode in thin samples mirrored that of thicker counterparts in both environments. A distinct observation was the

intermittent nature of crack growth, which resulted in striations on the fractured surface, with hydrogen environments exhibiting shorter striation spacings. Beneath these fracture surfaces, deformation microstructures remained consistent in both settings, revealing three layers, each defined by unique plastic strain gradients and dislocation densities. The hydrogen environment invoked the hydrogen-enhanced localized plasticity (HELP) mechanism, which is postulated to influence crack growth. The presence of hydrogen also led to variations in the characteristics of these layers, like the magnitude of plastic strain and dislocation structure, when compared to the air environment. Another intriguing observation was the reverse plastic deformation in regions trailing the crack front during its growth. This phenomenon is hypothesized to both increase the crack tip opening angle (CTOA) and aid in the crack tip's blunting.

R.Pandiyarajan et al. (2021) [16] This study presents a fatigue life and fatigue crack growth rate analysis of large diameter ball bearing under cyclic loading condition by using numerical and experimental methods. The large diameter of ball bearing was made up of high strength low alloy steel (42CrMo4), and the two dimensional finite element analysis (FEA) is used to predict the minimum life of ball bearing and validated by using of Basquin's relationship in the numerical study method, and its fatigue crack propagation is numerically and experimentally investigated. The specimen, notch preparation, and testing methods are performed according to ASTM-E647 standard in the experimental method. The crack propagation is found by experimentally, and the results are applied in the Paris equation for find the crack growth rate and stress intensity factor (delta-K) under the high cycle fatigue life loading by using of the mathematical relationship of da/dN = C(ΔK)n in the prediction. The predicted results are correlated with the experimental test results of 42CrMo4 material used large diameter ball bearings.

R.S. Neves et al. (2020) [21] In this comprehensive research, we introduce an innovative, incremental methodology for predicting the fatigue life of ductile materials, especially when they are under the influence of low cycle fatigue. This method uniquely departs from traditional life prediction models. At its core, this method hinges on monitoring the progressive evolution of an internal damage variable. What makes our approach distinct is its foundation on an extended version of the well-regarded Gurson model. This extended model is adept at capturing the nuanced, gradual deterioration of materials as they undergo successive loading cycles. As materials are cyclically stressed, they invariably exhibit signs of wear and fatigue. Our method offers a more refined lens through which we can observe and quantify this degradation. By tracking these internal changes, we aim to provide a more accurate and dynamic estimate of a material's remaining service life under conditions of low cycle fatigue. This approach, we believe, can greatly enhance the reliability and safety margins of structures and components crafted from ductile materials, ensuring their longevity and optimal performance throughout their lifecycle.

III. OBJECTIVE

The current research investigates the effect of elliptical crack on cylindrical bar using Finite Element Analysis (FEA) on fatigue life, stress and strain. The stress life approaches used for analysis.

- Developing CAD model of cylindrical bar with elliptical crack.
- Structural analysis of cylindrical bar under axial and torsional loading conditions.
- Changing elliptical crack dimensions (a/c ratio) and reconducting FEA analysis under same loading conditions. Here '*a*' is depth of crack and '*c*' is half width of crack.
- Determining stress, strain, fatigue life using stress life approach.
- Comparative analysis on the basis of above stated parameters.

IV. MWTHODOLOGY

Mathematical and finite element analyses for elliptical crack on cylindrical bar at different crack orientation angle such as 0 degree to 40 degree have been used. The structural and fatigue analysis have been performed for different design of elliptical crack on cylindrical bar in order to find out minimum fatigue life cycle, von mises stresses and factor of safety. For that total five designs of elliptical crack on cylindrical bar created.

Stress ratio effect

Cycles with higher stress ratio

$$R = \frac{K_{min}}{K_{max}} = \frac{P_{min}}{P_{max}}$$

Have an increased rate of crack growth. This effect is often explained using the crack closure concept which describes the observation that the crack faces can remain in contact with each other at loads above zero. This reduces the effective stress intensity factor range and the fatigue crack growth rate.

Crack closure is a phenomenon in fatigue loading, where the opposing faces of a crack remain in contact even with external load acting on the material.

As the load is increased, a critical value will be reached at which time the crack becomes open. Crack closure occurs from the presence of material propping open the crack faces and can arise from many sources including plastic deformation or phase transformation during crack propagation, corrosion of crack surfaces, presence of fluids in the crack, or roughness at cracked surfaces.

4.1 Estimate of fatigue life

The estimate of fatigue life can be made by integrating the Paris crack growth law, if the Stress Intensity Factor range is within the second region, the linear region

$$\int_{N_o}^{N_f} dN = \int_{a_o}^{a_f} \frac{da}{C(\Delta K)^n}$$

The above equation can be used to determine either how many fatigue cycles, $N_f - N_o$ are required to take for the crack, a_o to reach a certain size, a_f or how large crack is reached for a fixed number of loading cycles.

4.2 Sequence effects

A $\frac{da}{dN}$ equation gives the rate of growth for a single cycle, but when the loading is not constant amplitude, changes in the loading can lead to temporary increases or decreases in the rate of growth.

When a loading sequence experiences an overload, the rate of crack growth tends to decelerate. Such overloads lead to the formation of a plastic zone, which can act as an impediment, stalling the crack's advancement. This plastic deformation around the crack tip can introduce compressive residual stresses, which in turn serve as barriers to crack propagation. The significance of understanding this delay is vital, as it plays a crucial role in determining the overall lifespan of materials subjected to cyclic loading. The nature of these delays can be elucidated by various mathematical representations. Among them, two prominent equations stand out as especially effective tools for simulating the delays a crack encounters as it traverses the region impacted by an overload. These equations provide invaluable insights into the intricate interplay of material behavior, loading conditions, and resultant crack dynamics.

The Wheeler model (1972)

$$\left(\frac{da}{dN}\right)_{VA} = \beta \left(\frac{da}{dN}\right)_{CA} \quad where\ \beta = \left(\frac{r_{pi}}{r_{max}}\right)^k$$

Where

r_{pi}= plastic zone corresponding to the i_{th} cycle that occurs post the overload

r_{max}= distance between the crack and the extent of the plastic zone at the overload

VA = Variable amplitude

CA = Constant amplitude

The Willenborg model [Jiang Shan at el. 2016]

$$\frac{da}{dN} = C_F \frac{(\Delta K_{eff})^{mF}}{(1 - R_{eff})K_c - \Delta K_{eff}}$$

Where

$$\Delta K_{eff} = \frac{K_{min,eff}}{K_{max,eff}}$$

C_F & m_F are calibration parameters obtained under constant amplitude loading,

K_c= Critical stress intensity factor, and

K_{eff}= Effective stress ratio

- *Threshold equation*

Used to predict the crack growth rate at the near threshold region,

$$\frac{da}{dN} = A(\Delta K - \Delta K_{th})^P$$

- *Paris–Erdoğan equation*

Used to predict the crack growth rate in the intermediate regime and defines the straight-line region of crack growth. It does not account for the stress ratio R. Because the crack growth rate in a material is dependent on the stress ratio, if the Paris equation is to be used for a non zero stress ratio then an appropriate value of C will need to be used for the stress ratio R of interest.

$$\frac{da}{dN} = C(\Delta K)^m$$

4.3 Dimensional parameter and specification of cylindrical shaft with different cracks profile The cylindrical model has diameter D = 10 mm and length L = 80 mm. Displacement constraints in x, y and z directions are applied on either end of the cylindrical model. Meanwhile, a combination of axial and torsional stresses is applied on another end. A semi-elliptical surface crack was introduced at the mid-length of the model. The crack plane is set to be normal to the axis of the round bar.

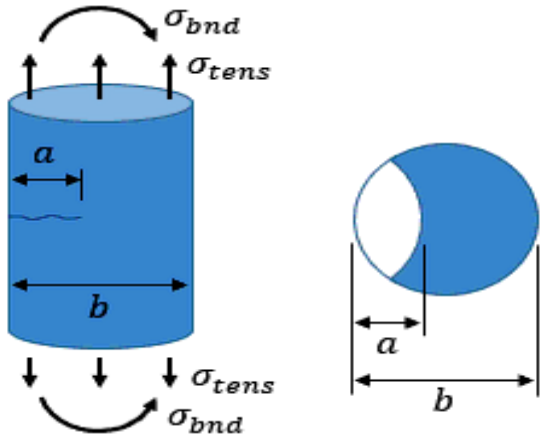

Figure 6 Cylindrical model with crack

The crack-shaping region of the specimen to have a semi-circular or semi-elliptical shape (a/c = 1 = 1 mm/1 mm and a/c = 2 = 1 mm/ 0.5 mm as shown in Figure.

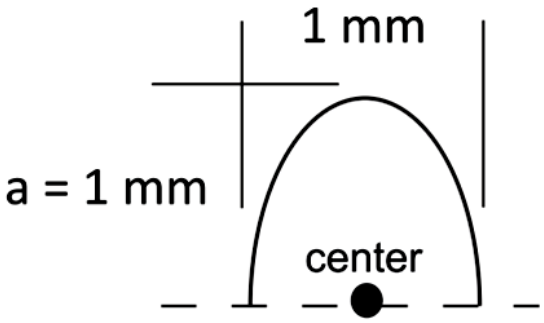

Figure 7 Crack-shaping region of the specimen

The mechanical and fracture characteristics of Al-6061-T6, utilizing the NASGRO constants/parameters, are sourced from the research by D. Chandra et al. (2016). Employing the NASGRO crack propagation formula, a stress ratio, R, is set at 0. The numerical simulation delineates the trajectory of crack growth over an estimated number of cycles, with a/c set at 1. This is conducted under a combined cyclic loading, where tension is alternately set at 100 MPa and 125 MPa, and torsion is fixed at 100 MPa.

Table 1 Mechanical and fracture properties of 6061-T6 aluminum alloy *[D. Chandra at el. (2016)]*

Material properties	**Values**
Modulus of elasticity (GPa)	69
Poisson's ratio	0.33
Yield stress (0.2 %) (MPa)	282.69
Ultimate tensile strength (MPa)	310.26
Plane stress fracture toughness, KC (MPa$\sqrt{}$mm)	1250.95
Plane Strain fracture toughness, KIC (MPa$\sqrt{}$mm)	903.46
Crack growth rate coefficient (C)	6.53E-10
NASGRO N exponent (N)	2.3
NASGRO P coefficient (P)	0.5
NASGRO Q coefficient (Q)	0.5
Threshold SIF range at R = 0 (ΔK_{th}) (MPa$\sqrt{}$mm)	121.62
Plane stress/strain constraint factor, α	2.0
S_{max}/S_0	0.3

Cylindrical cracks represent a critical challenge in the domain of engineering structures, necessitating advanced methodologies for detection, prevention, and mitigation. This review emphasizes the pivotal role of effective coating layers and self-healing mechanisms in reducing stress intensity factors, enhancing component durability, and ensuring fuel economy. Additionally, the paper highlights the significance of cutting-edge non-destructive testing techniques, including Ultrasonic Testing, Eddy Current Testing, and Radiographic. Testing, and Infrared Thermography, for accurate crack characterization. By amalgamating these approaches, engineers can make informed decisions, mitigate structural risks, and ensure the long-term safety and reliability of cylindrical components across diverse industrial applications. Future research endeavors should focus on refining these techniques and exploring innovative materials and technologies to further advance the field of crack management in engineering structures.

4.4 Algorithm used for Finite element analysis of Structural and fatigue analysis

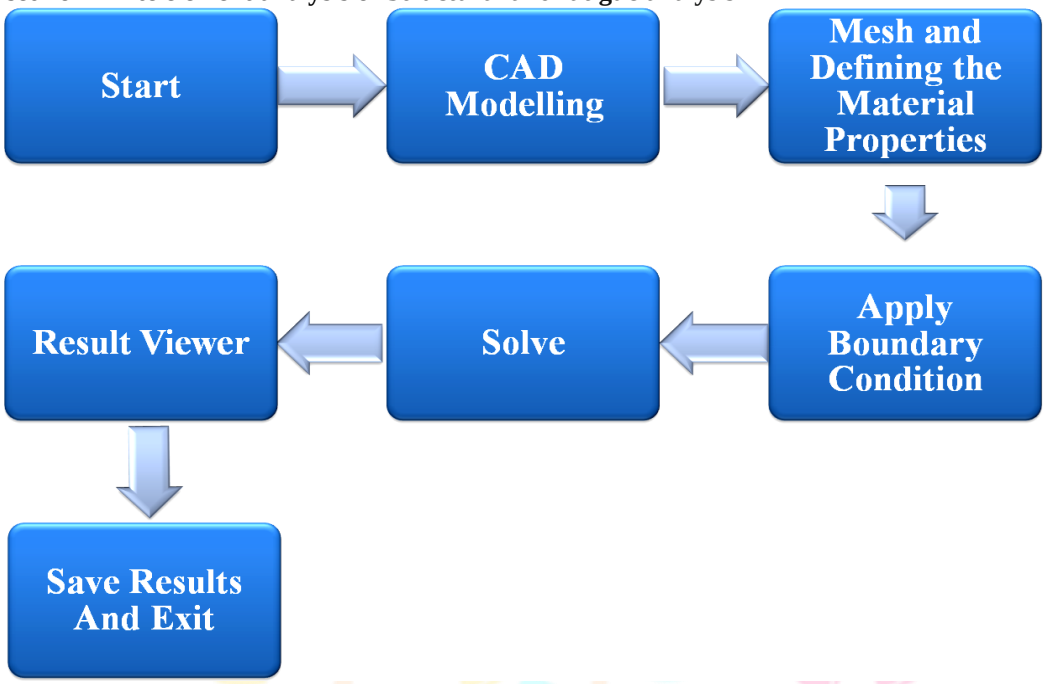

Figure 8 Algorithm used for Finite element analysis of Structural and fatigue analysis

4.5 Grid independent test

Grid independent is associated with the accuracy or even rationality of numerical results. Grid-independent means calculation results change so little along with a denser or looser grid that the truncation error can be ignored in numerical simulation. Whether the grid is independent directly influences the truncation error or even the rationality of numerical results. When considering grid-independent test, a very dense grid can avoid this problem but the calculation resource may be wasted unnecessarily. In practice, we usually increase the grid resolution according to a certain ratio and then compare the results of two neighborhood results. If the results tend towards identical the grid can be considered as grid-independent. Such strategy can utilize computational resource most efficiently as well as obtain reasonable results.

Table 2 Element Size Impact: Stress and Fatigue Analysis

S. No.	Element size	No. of elements	Equivalent Stress [MPa]	Min. Life [Cycle]
1	Default	63949	217.99	11773
2	1 mm	140553	226.86	11673
3	0.75 mm	175033	226.85	11579
4	0.5 mm	192667	226.32	11496
5	0.25 mm	368222	226.31	11490

The current research investigates the effect of elliptical crack on cylindrical bar using Finite Element Analysis (FEA) on equivalent stress and minimum fatigue life have been checked how numerical result converges when refining computational grid as shown in figure 9.

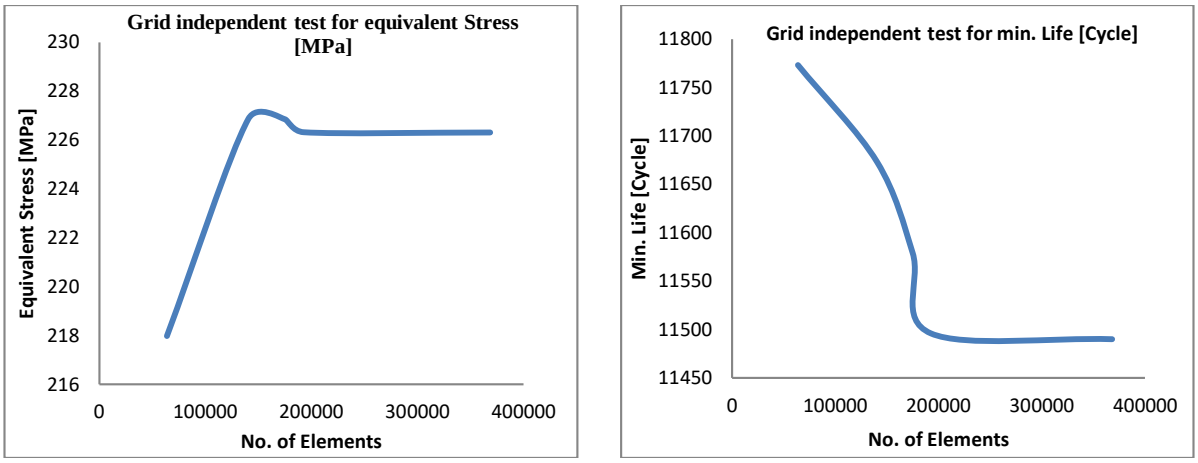

Figure 9 Grid independent test for equivalent Stress & minimum life cycle

Boundary Conditions

1. Create CAD model of elliptical crack on cylindrical bar of different design at different orientation (0^o, 10^o , 20^o , 30^o & 40^o)
2. Apply fixed support at the one end of the elliptical crack on cylindrical bar.
3. Apply Pressure and moment at another end bending = 100 Mpa, torsion =100 Mpa for case-1 and bending = 100 Mpa, torsion =125 Mpa for case-1 which includes force and displacement support.
4. Check von misec or equivalent stress as an output.
5. Check minimum life of the elliptical crack on cylindrical bar by using fatigue tool.
6. Check minimum and maximum factor of safety of elliptical crack on cylindrical bar by using fatigue tool.
7. After applying boundary conditions solve the model using APDL solver and compare the equivalent stress, life and factor of safety of the elliptical crack on cylindrical bar.

V. RESULT AND DISCUSSION

Mathematical and finite element analyses for elliptical crack on cylindrical bar at different crack orientation angle such as 0 degree to 40 degree have been used. The structural and fatigue analysis have been performed for different design of elliptical crack on cylindrical bar in order to find out minimum fatigue life cycle, von mises stresses and factor of safety. For that total five designs of elliptical crack on cylindrical bar created of different design at different orientation (0^o, 10^o, 20^o, 30^o & 40^o), fixed support at the one end and Pressure and moment at another end. After applying boundary conditions solve the model using APDL solver and compare the equivalent stress, life and factor of safety of the elliptical crack on cylindrical bar. In this chapter result and discussion have been explained using various contours, table and graphical representation.

Table 3 Comparative results of Structural and fatigue analysis for elliptical crack on cylindrical bar

Design Parameters	Load Parameters	Equivalent Stress [Mpa]	Minimum Life [Cycles]	Factor of Safety	
				Min.	Max
Design-1 (Crack orientation Angle 0^o)	Load Case-1 (tension = 100 Mpa, torsion =100 Mpa)	226.32	11496	0.366	4.140
	Load Case-2(tension = 100 Mpa, torsion =125 Mpa)	342.78	3106.6	0.2412	1.485
Design-2 (Crack orientation Angle 10^o)	Load Case-1 (tension = 100 Mpa, torsion =100 Mpa)	247.86	12092	0.347	3.41
	Load Case-2(tension = 100 Mpa, torsion =125 Mpa)	387.53	2982.3	0.222	1.434
Design-3 (Crack orientation Angle 20^o)	Load Case-1 (tension = 100 Mpa, torsion =100 Mpa)	208.47	22015	0.413	3.410
	Load Case-2(tension = 100 Mpa, torsion =125 Mpa)	337.12	4587.7	0.255	1.364
Design-4 (Crack orientation Angle 30^o)	Load Case-1 (tension = 100 Mpa, torsion =100 Mpa)	216.46	19233	0.398	3.410
	Load Case-2(tension = 100 Mpa, torsion =125 Mpa)	355.6	3890.1	0.242	1.384

Design-5 (Crack orientation Angle 40°)	Load Case-1 (tension = 100 Mpa, torsion =100 Mpa)	218.59	18599	0.394	3.41
	Load Case-2(tension = 100 Mpa, torsion =125 Mpa)	363.3	3641	0.237	1.364

5.1 Comparative results of Structural and fatigue analysis for elliptical crack on cylindrical bar for Load case-1

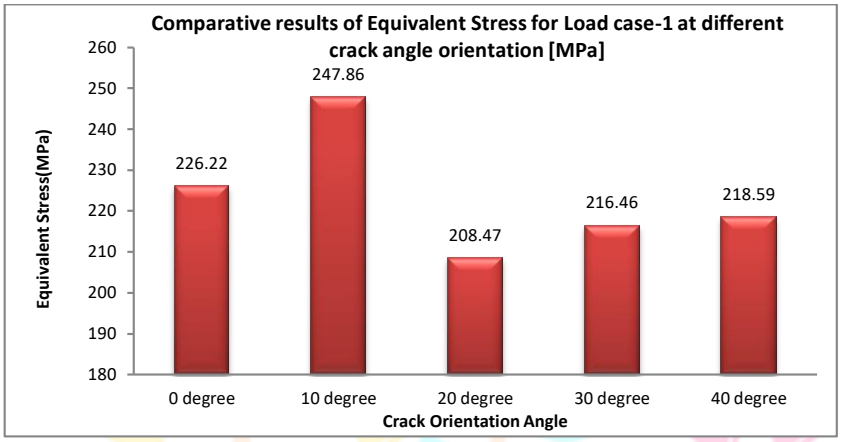

Figure 10 Comparative results of Equivalent Stress for Load case-1 at different crack angle orientation

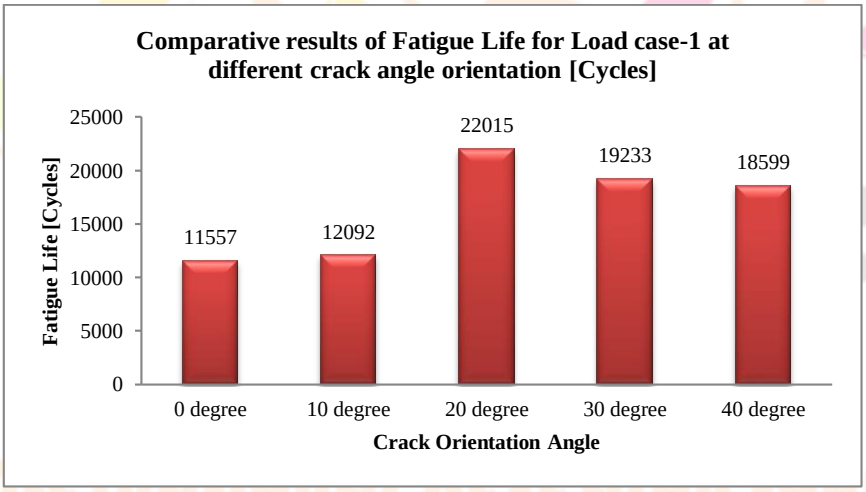

Figure 11 Comparative results of Fatigue Life for Load case-1 at different crack angle orientation

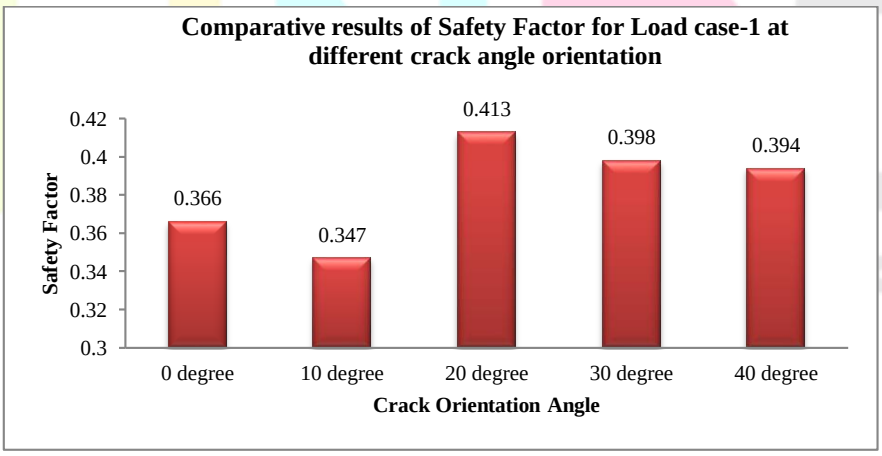

Figure 12 Comparative results of Safety Factor for Load case-1 at different crack angle orientation

and minimize contact pressures between mating spur gear teeth, specifically by adjusting the spur gear's face width. Utilizing CATIA, three distinct CAD models for the driving gear were conceptualized. Post design, these were converted into the Stp. format to facilitate in-depth analysis. The inaugural design, Design-1, was derived from dimensional parameters extracted from a foundational paper. Meanwhile, Design-2 hinged on mathematically determined parameters rooted in the gear module. In a bold approach, Design-3 was contrived by amplifying the geometrical parameters by a substantial 20% compared to the original base design. Each of these designs underwent rigorous evaluations encompassing steady-state structural scrutiny, fatigue analysis, and

contact dynamics assessment. This chapter delves deep into the findings of the finite element model analysis, elucidating results through comprehensive visual aids like contour plots and illustrative graphs.

Table 4 Comparative results of spur gear assembly for design-1

Torque [N_m]	Von-mises stress [MPa]	Min. Life [Cycle]	Safety Factor	Max Life [Cycle]	Hysteresis Stress [MPa]	Hysteresis Strain [mm/mm]	Contact Pressure [MPa]	Penetration [mm]
350	919.99	65861.0	0.1838	1.47E+6	389.18	0.0109	447.21	0.0188
400	1048.60	38734.0	0.1613	7.76E+5	408.74	0.0135	508.98	0.0214
450	1177.40	24439.0	0.1437	4.52E+5	426.53	0.0163	570.77	0.0240
500	1306.20	16270.0	0.1295	2.83E+5	442.92	0.0193	632.56	0.0266
550	1435.10	11301.0	0.1179	1.87E+5	458.16	0.0225	694.36	0.0290
600	1564.20	8123.6	0.1081	1.30E+5	472.42	0.0259	756.17	0.0318

Table 5 Comparative results of spur gear assembly for design-2

Torque [N_m]	Von-mises stress [MPa]	Min. Life [Cycle]	Safety Factor	Max Life [Cycle]	Hysteresis Stress [MPa]	Hysteresis Strain [mm/mm]	Contact Pressure [MPa]	Penetration [mm]
350	1092.80	34768.0	0.1550	6.72E+5	412.77	0.0140	581.41	0.02100
400	1249.70	20478.0	0.1356	3.63E+5	433.51	0.0174	658.50	0.02379
450	1406.80	12932.0	0.1204	2.16E+5	452.40	0.0211	735.61	0.02657
500	1564.10	8613.9	0.1083	1.37E+5	469.80	0.0252	812.74	0.02936
550	1721.50	5984.6	0.0984	91617	485.99	0.0295	889.89	0.03214
600	1879.00	4302.3	0.0902	63913	501.15	0.0340	of 967.06	0.03490

Table 6 Comparative results of spur gear assembly for design-3

Torque [N_m]	Von-mises stress [MPa]	Min. Life [Cycle]	Safety Factor	Max Life [Cycle]	Hysteresis Stress [MPa]	Hysteresis Strain [mm/mm]	Contact Pressure [MPa]	Penetration [mm]
350	838.74	1.02E+05	0.2020	2.47E+06	373.71	0.0091	397.24	0.0190
400	946.57	61985.0	0.1790	1.34E+06	391.29	0.0111	448.64	0.0220
450	1054.50	40086.0	0.1607	7.94E+05	407.37	0.0132	500.05	0.0240
500	1162.50	27211.0	0.1457	5.04E+05	422.24	0.0155	551.47	0.0265
550	1270.50	19200.0	0.1334	3.37E+05	436.11	0.0179	602.90	0.0290
600	1378.70	13982.0	0.1229	2.35E+05	449.13	0.0204	654.33	0.0315

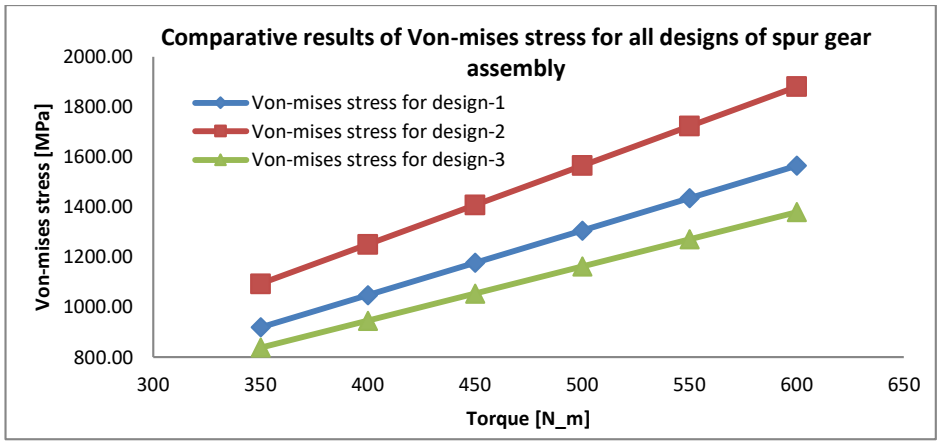

Figure 13: Comparative results of Von-mises stress for all designs of spur gear assembly

Based on the comparison of Von-Mises stress in the spur gear assembly, design-3 exhibits a reduction in equivalent stress by 9.69% at 350 N m and 13.45% at 600 N m relative to design-1.

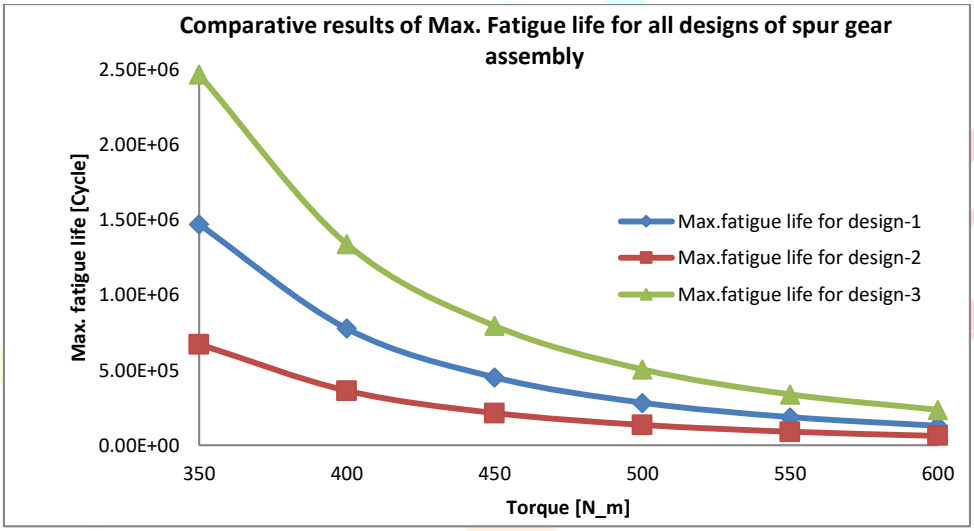

Figure 14: Comparative results of Max. Fatigue life for all designs of spur gear assembly

Based on the comparative analysis of maximum fatigue life within the spur gear assembly, design-3 demonstrates an increase in fatigue life of 67.7% at 350 N m and 81.59% at 600 N m compared to design-1.

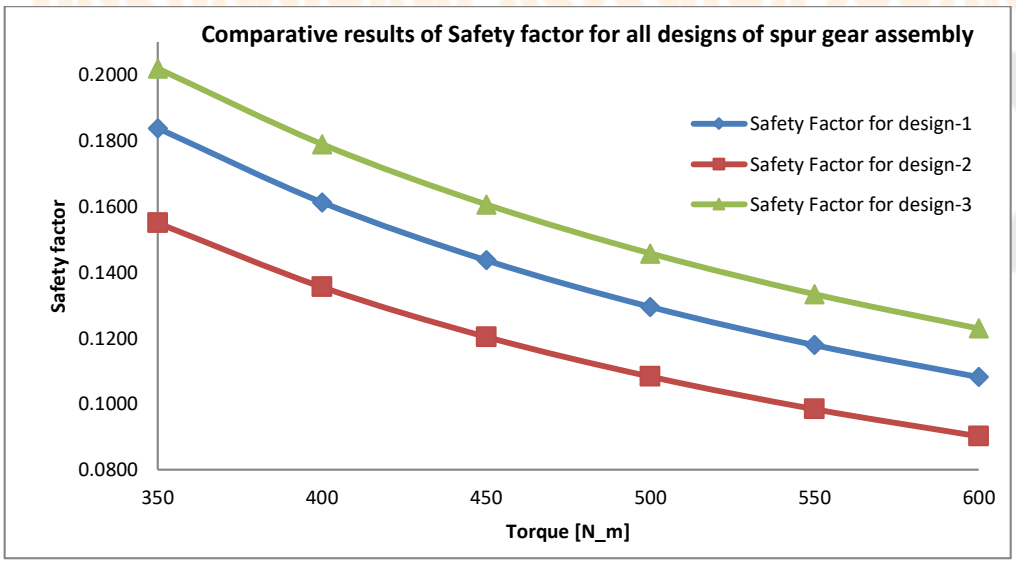

Figure 15: Comparative results of Safety factor for all designs of spur gear assembly

Based on the comparison of the safety factor in the spur gear assembly, design-3 showcases an enhanced safety factor by 9.88% at 350 N m and 13.65% at 600 N m compared to design-1.

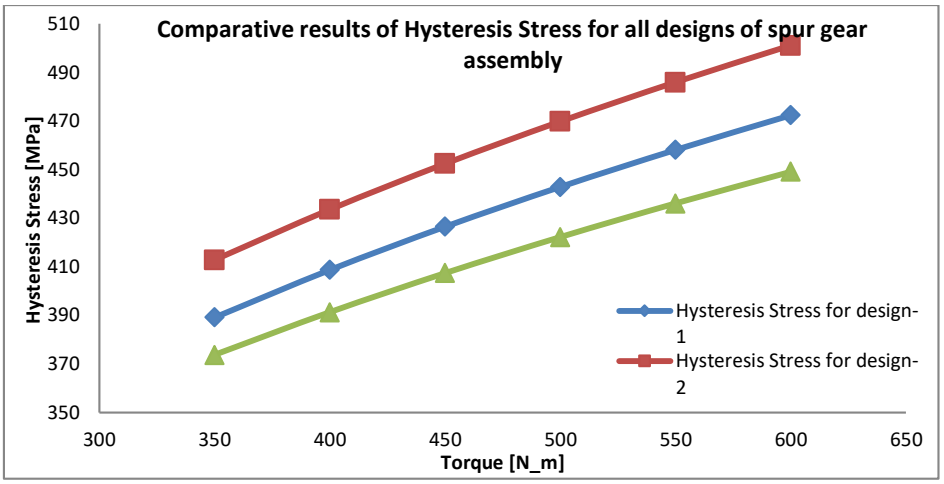

Figure 16: Comparative results of Hysteresis Stress for all designs of spur gear assembly

Based on the Hysteresis stress comparison within the spur gear assembly, design-3 exhibits a decrease of 4.14% at 350 N m and 5.19% at 600 N m relative to design-1.

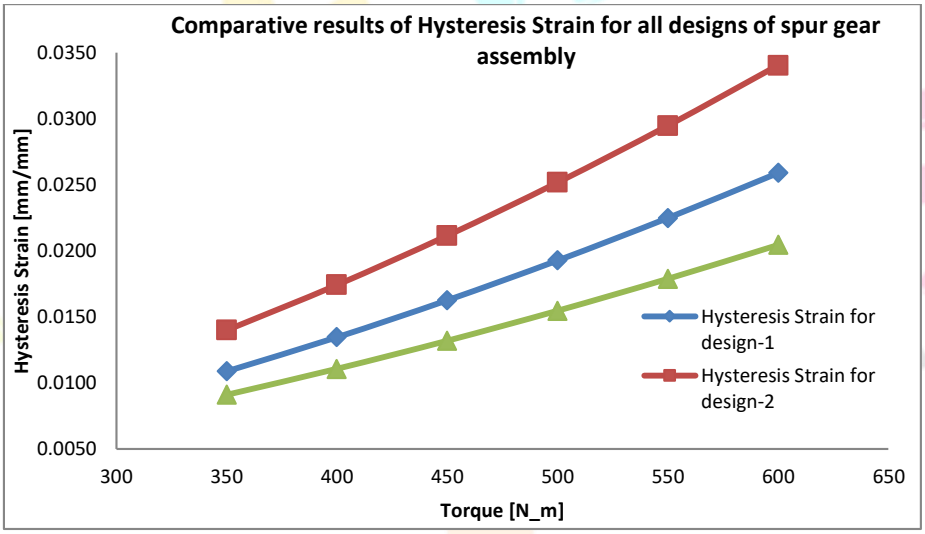

Figure 17: Comparative results of Hysteresis Strain for all designs of spur gear assembly

When comparing the Hysteresis strain in the spur gear assembly, design-3 demonstrates a reduction of 19.58% at 350 N m and 26.63% at 600 N m compared to design-1.

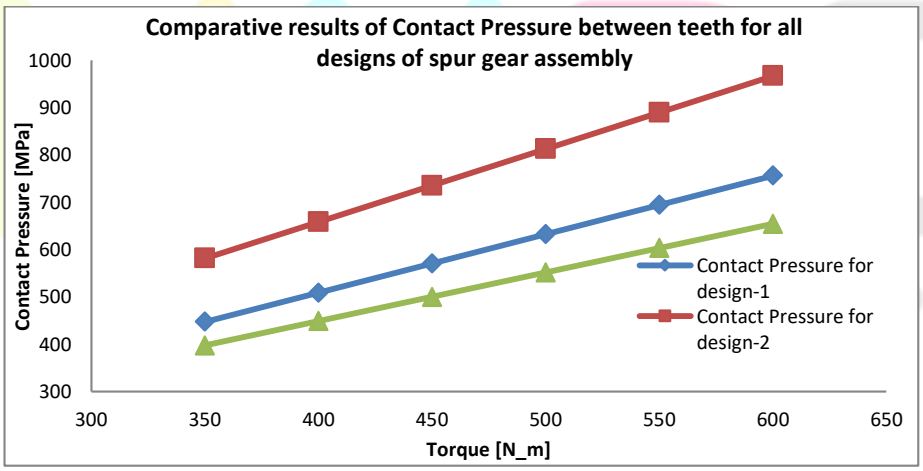

Figure 18: Comparative results of Contact Pressure between teeth for all designs of spur gear assembly

Based on the comparative analysis of the Contact Pressure between the teeth of the spur gear assembly, design-3 exhibits a reduction of 12.58% at 350 N m and 15.56% at 600 N m relative to design-1.

From the above Comparative results of Structural and fatigue analysis for elliptical crack at different orientation (Design-1 to design-5) on cylindrical bar for Load case-2 as shown in figure 00-00. It has been observed that as the crack orientation has changed the equivalent stress also changed, for the crack orientation 10 degree the maximum equivalent stress is 343.78 MPa while for the crack orientation 20 degree the maximum equivalent stress is 387.53 MPa, for the crack orientation 30 degree the value of equivalent stress is 337.12 MPa which is minimum in all designs and increasing for orientation angle 30 and 40 degree.

Comparative result of fatigue life for load case-2 shows that the minimum fatigue life of 2982.3 cycle occurs at 10 degree and the maximum fatigue life 4587.7 cycle at 20 degree crack orientation for design 3 (20 degree) and for crack orientation 30 degree and 40 degree the fatigue life cycle decreasing gradually as compared with design-3.

Safety factor at 0 degree crack orientation is greater than of 10 degree, the maximum factor of safety 0.225 at 20 degree and from design 4 and 5 where crack orientation is 30 degree and 40 degree decreasing slightly as compared from desin-3.

It has been observed that equivalent stresses increased for design-4 & design-5 while fatigue life (19233 & 18599) as compared with design-1 and safety factor decreasing from design-3 to design-5 (0.255, 0.2424 & 0.237).

6. CONCLUSION

This study provides a comprehensive analysis of crack growth in cylindrical bars, offering valuable insights into the intricate mechanisms governing this phenomenon. Through extensive Finite Element Analysis and mathematical modeling, the research explores the impact of crack orientation angles, stress ratios, and loading sequences on crack behavior. The findings underscore the importance of understanding crack closure phenomena and employing advanced coating layers and self-healing mechanisms to mitigate structural risks. The integration of non-destructive testing techniques proves instrumental in accurately characterizing cracks. By amalgamating these approaches, engineers can make informed decisions, enhance component durability, and ensure the long-term safety and reliability of cylindrical structures in various industrial applications. Future research efforts should continue to refine these techniques and explore innovative materials and technologies to further advance the field of crack management in engineering structures.

REFERENCES

[1] Yu, Y., Kurian, B., Zhang, W., Cai, C. S., & Liu, Y. 2021. Fatigue damage prognosis of steel bridges under traffic loading using a time-based crack growth method. Engineering Structures, 237, 112162. doi:10.1016/j.engstruct.2021.112162

[2] Xu, Z. K., Wang, B., Zhang, P., & Zhang, Z. F. 2021. Short fatigue crack growth behavior in 18Ni marageing steel. Materials Science and Engineering, 807, 140844. doi:10.1016/j.msea.2021.140844

[3] Williams, W. M., Shabani, M., Jablonski, P. D., & Pataky, G. J. 2021. Fatigue crack growth behavior of the quaternary 3d transition metal high entropy alloy CoCrFeNi. International Journal of Fatigue, 148, 106232. doi:10.1016/j.ijfatigue.2021.106232

[4] Pettit, R. G.. 2021. Crack growth threshold testing with flat-bottom hole specimens and artifact evaluation of electrothermal crack tip marking. Engineering Fracture Mechanics, Available online 20, 249, 107737. doi:10.1016/j.engfracmech.2021.107737

[5] Kumar, K., Bhadauria, S. S., & Singh, A. P. 2021. Finite element analysis of crack initiation and growth in a rectangular plate with pre-existing pits. Materials Today: Proceedings, 44(2), 3050–3054. doi:10.1016/j.matpr.2021.02.442

[6] Jape, S., Young, B., Haghgouyan, B., Hayrettin, C., Baxevanis, T., Lagoudas, D. C., & Karaman, I. 2021. Actuation-Induced stable crack growth in near-equiatomic nickel-titanium shape memory alloys: Experimental and numerical analysis. International Journal of Solids and Structures, 221, 165–179. doi:10.1016/j.ijsolstr.2020.09.032

[7] Huynh, T. T., Hamada, S., Tsuzaki, K., & Noguchi, H. 2021. Roles of hydrogen and Plastic Strain Distribution on Delayed Crack Growth in Single-crystalline Fe–Si alloy. Materials Science and Engineering, 803, 140703. doi:10.1016/j.msea.2020.140703

[8] Pandiyarajan, R., Arumugam, K., Prabakaran, M. P., & Vetrivel kumar, K. 2021. Fatigue life and fatigue crack growth rate analysis of high strength low alloy steel (42CrMo4). Materials Today: Proceedings, 37(2), 1957–1962. doi:10.1016/j.matpr.2020.07.486

[9] Neves, R. S., Ferreira, G. V., & Malcher, L. 2020. Gurson-based incremental damage in fatigue life estimate under proportional and non-proportional loading: Constant amplitude and low cycle regime applications. Theoretical and Applied Fracture Mechanics, 108. doi:10.1016/j.tafmec.2020.102678

[10] Joseph, R. P., Putra, I. S., Darmawan, A. S., Liew, H. L., Ramesh, S., . . . Purbolaksono, J. 2020. Fracture analysis of a corner crack in a pinhole of a solid cylinder under torsion loading. Engineering Solid Mechanics, 8, 353–364. doi:10.5267/j.esm.2020.3.003

[11] Geng, M., Chen, H., Yang, Y., & Li, Y. 2020. Prediction of crack shape in a cylindrical bar under combined fatigue tension and torsion loading. Theoretical and Applied Fracture Mechanics, 109, 102727. doi:10.1016/j.tafmec.2020.102727

[12] Pokrovskii, A. M., Dubin, D. A., & Vdovin, D. S. 2019. Fatigue-crack propagation in torsional shafts within the suspension of high-speed caterpillar vehicles. Russian Engineering Research, 39(7), 548–555. doi:10.3103/S1068798X19070165

[13] Ntritsos, D. G., Tsolakis, A. D., & Giannakopoulos, K. I. 2018. Experimental and analytical approach of fatigue behaviour of stepped CK45 shaft with adjacent key groove. Procedia Structural Integrity 1st International Conference of the Greek Society of Experimental Mechanics of Materials, 10, 288–294. doi:10.1016/j.prostr.2018.09.040